Step-step interaction on vicinal Si(001) surfaces studied by scanning tunneling microscopy

L. Persichetti, A. Sgarlata, M. Fanfoni, M. Bernardi, and A. Balzarotti
Dipartimento di Fisica, Università di Roma "Tor Vergata," Via della Ricerca Scientifica, 1-00133 Roma, Italy
(Received 18 May 2009; revised manuscript received 15 July 2009; published 21 August 2009)

We report on measurements of step-step interaction on a flat Si(111)-(7×7) surface and on vicinal Si(001) surfaces with miscut angles ranging between 0.2° and 8°. Starting from scanning tunneling microscopy images of these surfaces and describing steps profile and interactions by the continuum step model, we measured the self-correlation function of single steps and the distribution of terrace widths. Empirical parameters, such as step stiffness and step-step interaction strength, were evaluated from the images. The present experiment allows to assess the dependence of the step-step repulsion on miscut angle, showing how parameters drawn from tunneling images can be used to interpolate between continuum mesoscopic models and atomistic calculations of vicinal surfaces.

DOI: 10.1103/PhysRevB.80.075315 PACS number(s): 68.35.B−, 81.05.Cy, 68.37.Ef

I. INTRODUCTION

Surface steps are key microstructural features of great interest in surface physics and surface growth processes. Steps can be inherently present on surface or introduced in excess through a miscut angle as in vicinal surfaces, either way their presence affects almost any fabrication process at the nanoscale. By periodically modulating the topology of the surface, steps lend themselves to function as natural templates for overlayers growth, thus exerting a range of roles in the self-assembly and nanoscale evolution of materials surfaces.[1] In this regard, steps are able to impart nanoscale, mesoscale, and macroscale ordering and alignment to deposited inorganic[2] and organic[3,4] thin films, enabling a careful tailoring of substrates of technological relevance. The control of the steps morphology through step bunching, faceting, annealing, and alloying[5,6] has been widely adopted to prepare nanostructures on metals[7] and semiconductors.[8–10] In this latter category, Si(001) and Si(111) vicinal surfaces have been used extensively to the scope.[11] Apart from being fascinating for their technological potential, surface steps certainly constitute an area of focus of modern surface physics.

A range of atomistic and continuum models have been developed to explain physical properties and phenomena in which steps are involved and comprehensive reviews of these efforts have been written.[12,13] In this paper, we concentrate our attention on the Si(001) and its vicinal surfaces that due to the wide range of featured surface phenomena are considered a versatile model system.[14]

The Si(001) surface displays a (2×1) reconstruction with rows of dimerized atoms. The dimers direction is orthogonal on terraces separated by an odd number of single-height steps and this results in an alternation of (2×1) and (1×2) domains in the case where single steps are solely present. Following a standard convention first introduced by Chadi,[15] we define S_A and S_B steps as those in which the upper-terrace-dimerization direction is perpendicular or parallel to the step ledge, respectively. S_A steps contain few kinks, have a smooth profile, and run almost perpendicular to the upper-terrace-dimer-bond direction while the S_B-steps profile is relatively wavy due to the higher concentration of kinks.

On vicinal surfaces with low miscut angle ϕ, the two types of steps alternate and as the miscut angle is increased, an evolution to a surface made up mostly of double-height steps (D_B steps) is observed. D_B steps occur without change in the upper-terrace reconstruction and for energetic reasons are rebonded up to a miscut angle of $\phi \approx 11°$.[16]

The transition from single to double steps has been characterized both experimentally[14,17,18] and theoretically.[19,20] Pehlke *et al.* described this transition as a chemical equilibrium between two phases S_A+S_B and D_B, leading to a reaction $S_A+S_B \rightarrow D_B$ that proceeds rightward as the miscut angle increases. In doing so, the single steps S_A and S_B gradually merge to double steps. During this transition, large domains of the two individual phases (S_A+S_B and D_B) are not observed and a fairly continuous alternation of the two is rather formed at the surface.[18,20] An explanation of this behavior was given in terms of interactions of elastic steps monopoles and dipoles,[21] accounted for by an effective one-dimensional (1D) Hamiltonian. This model successfully predicted the average measured terrace-width distributions (TWDs) at terraces of small and intermediate size.[22]

Within this framework, we devoted our efforts to analyze the step-height evolution of Si(111) and of Si(001) vicinal surfaces with different miscut angles ϕ between 0.2° and 8° since it is known that the step-height transition should occur beyond $\phi=2°$.[19,20,22,23] By means of scanning tunneling microscopy (STM), we assessed the terrace-width distribution on a large set of images, extrapolating from them the step stiffness and the relevant step-step interaction parameters. Our investigation provides support to the picture of intermixing between single- and double-height steps on vicinal Si(001) surfaces when the misorientation angle is increased. The step stiffness is found to be an increasing function of ϕ and is explained in terms of the angle dependence of the step densities and of the terrace-step-kink (TSK) model. The step-step interaction strength, modeled for a simple binary solution, is a strongly decreasing function of ϕ at low angles and remains almost constant beyond approximately $\phi=2°$. All these findings are interpreted with the help of the elastic continuum model (CSM) (Ref. 24) and atomistic calculations.[20]

II. METHODOLOGY

At the steps length scale, CSM (Ref. 13) postulates that steps are the most relevant physical entities on the mesoscopic scale and a continuum approximation of their profile is made with an analytical function $x(y)$, where y is the coordinate running parallel to the step ledge and x is the coordinate of the step edge in the orthogonal direction for a given y. The TWD is obtained from the STM images by means of a statistical analysis of the step profiles. This image analysis largely follows standard methods.[24] A large collection of functions has been proposed for the TWD, each of them corresponding to different physical conditions at the surface, namely, the cases of attractive,[25] repulsive,[14,26] and noninteracting steps.[27] When the step-step repulsive interaction is dominant, a Gaussian distribution is usually adopted,[24] as resulting from a mean-field (Gruber-Mullins, GM) description of the surface.[28] TWD depends on three energy-related quantities, namely, (i) the thermal energy k_BT, which boosts steps fluctuations, (ii) the step stiffness $\tilde{\beta}$, inversely proportional to the step diffusivity, which opposes to steps bending,[24] and (iii) the strength A (or $\tilde{A}$), a parameter resulting from the functional form of the step-step repulsive interaction energy, $E(l)=Al^{-2}$, where l is the step-step distance or terrace width for a fixed y [i.e., $l=[x_1(y_0)-x_2(y_0)]$. k_B is the Boltzmann's constant and T is the surface freeze-in temperature and all the other parameters depend on ϕ. The step stiffness is measured from the fit of the mean-square step wandering spatial (self-) correlation function,[24] $G(y)=\langle[x(y)-x(0)]^2\rangle$, which increases linearly with y,

$$G(y) = \frac{k_BT}{\tilde{\beta}}y. \tag{1}$$

The linearity of the correlation function can be understood considering a random walker moving on either sides of neighboring steps while advancing in the y direction (which can be thought of as the time). As by definition $G(y)$ describes the average square net change in position along the direction explored by the walker, a linear dependence on the time y is expected. A relevant dimensionless combination of the aforementioned quantities is the modified interaction strength $\tilde{A}$, given by

$$\tilde{A} = \frac{A\tilde{\beta}}{(k_BT)^2}, \tag{2}$$

which is extracted directly from TWD. To this purpose, the standardized Gaussian distribution $\check{P}(s)=\frac{1}{\sigma\sqrt{2\pi}}\exp[-\frac{(s-1)^2}{2\sigma^2}]$, of $s=l/\langle l\rangle$ is considered. Within the Gaussian approximation an argument by GM (Refs. 24 and 28) shows that the variance in $\check{P}(s)$ depends on the approximation scheme used. A wide range of constants has been proposed[29] so that, for the sake of clarity, we report, in the following, σ^2 values calculated using

$$\sigma^2 = \frac{1}{\sqrt{48\hat{A}}}. \tag{3}$$

Nonetheless, the dependence of A on ϕ can be obtained from atomistic calculations of the step-step energy based on the Stillinger-Weber potential.[20] In these calculations the relaxed ledge energies $E(\phi)$ for flat and vicinal surfaces are computed on large periodic cells with terrace widths in the 1–30 nm range. The excess energies are then fitted to three coefficients describing the formation energy, the elastic stress-domain and the force-dipole interactions for single- and double-layer edges, along the lines described in Ref. 20. By means of these parameters one can determine the average ledge energy as

$$E(\phi) = E_S(\phi)n_S(\phi) + E_D(\phi)n_D(\phi), \tag{4}$$

where E_S and E_D are the equilibrium energies of pairs of S_A-S_B steps and D_B steps, respectively, and n_S and n_D are the relative densities of single S_A+S_B and double D_B steps. Since the repulsive interactions induced by the strain field and/or by dipoles scale as $\langle l\rangle^2$, we get $A(\phi)=E(\phi)\langle l\rangle^2$ as a function of ϕ.

III. EXPERIMENT

Experiments were carried out in an ultrahigh vacuum chamber with a base pressure $<5\times10^{-11}$ Torr, where an STM is available. Two kinds of samples were measured: n-type and P-doped Si(111) substrate slightly misoriented toward the $[-1,-1,2]$ direction and P-type B-doped Si(001) substrates misoriented toward the [110] direction from 0.2° to 8°. The nominal uncertainty on the offcut angle was ±0.5°. Samples were cleaned *in situ* by a standard flashing procedure at 1473 K and then they were annealed at the freeze-in temperature [1103 and 767 K for Si(111) and Si(001), respectively] in order to allow equilibration of the step structure. Further experimental details are reported elsewhere.[30] Images of the clean surfaces show almost no contamination from other species and little defect densities, as shown in Fig. 1 so that the defects do not influence the statistical analysis to be presented. For any STM image, the position of each step was sampled at intervals of 2 nm; the chosen sampling frequency was short enough to reconstruct exactly the step profile even in those areas where steps change between double and single height. At this point each step is coded by a discrete signal, to which a cubic spline curve is then accurately fitted in order to describe step profiles with proper $x(y)$ continuous functions. Step widths were calculated thereof for a significant statistical sample for each miscut angle and averaged over different regions of the sample; a full TWD was thus derived for each surface.

IV. RESULTS

A. Flat Si(111)-7×7 surface

In Fig. 2(a) a typical STM image of the flat Si(111) surface with monatomic steps is displayed. In Fig. 2(b) the related correlation function $G(y)$ is shown. The linear behavior

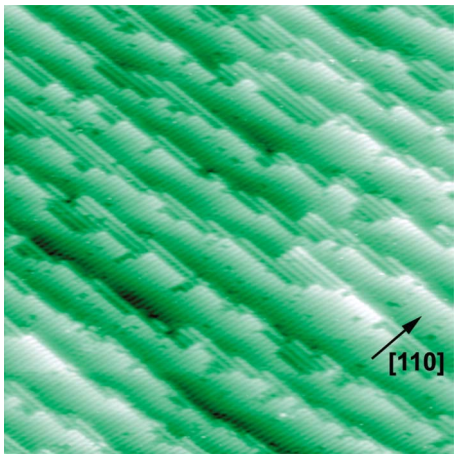

FIG. 1. (Color online) STM image (50×50 nm^2) of the clean 2°-off Si(001) surface. The [110] direction perpendicular to step edges is evidenced by the arrow.

is found over a y range much larger than the average step-step distance (approximately 46 nm) while for larger y values the linear dependence ceases, in qualitative agreement with theory.[24] The slope of $G(y)$ is evaluated to be 2.20 ± 0.02 Å, at the freeze-in temperature of $T=1103$ K. The step stiffness $\tilde{\beta}=43.2\pm0.4$ meV/Å is derived from the linear fit of $G(y)$ and compares well with reflection electron microscopy data at $T=1173$ K from which the value $\tilde{\beta}\approx46$ meV/Å is calculated.[26,31] The RMS and the average terrace width of the experimental $P(l)$ distribution, $P(l)=\frac{1}{w\sqrt{2\pi}}\exp[-\frac{(l-\langle l\rangle)^2}{2w^2}]$, are, respectively, $w=13\pm1$ nm and $\langle l\rangle=46\pm2$ nm. The related $\check{P}(s)$ distribution provides $\sigma^2=0.078\pm0.017$, from which we obtain $A=0.68\pm0.07$ eV Å. Making use of a more accurate expansion[29] for $\tilde{A}$, we calculate $A=0.46\pm0.02$ eV Å which agrees with the value $A=0.4\pm0.1$ eV Å measured by Williams *et al.*[32] Remarkably, A of the clean surface is between about two and three times smaller than that of a surface covered with 0.25 Å of Al, where A is measured to be 1.2 eV Å.[33] The present result confirms the previous finding that the step interaction energy is highly sensitive to submonolayer coverage of metals and provides a firm starting ground for the investigation of the vicinal Si(001) surfaces that we present in Sec. IV B.

B. Vicinal Si (001) surfaces

As an example of the analysis performed in the range of $\phi=0.2°-8°$, an STM image of a vicinal 4°-off Si(001) surface is shown in Fig. 3(a), along with the respective correlation function $G(y)$ in Fig. 3(b). The measured $\langle l\rangle$ as a function of ϕ is illustrated in Fig. 4 where, for the sake of comparison, a few data points measured on (1×2) terraces by Swartzentruber *et al.*[14] are included. In Fig. 5 we report the step stiffness $\tilde{\beta}$ as a function of ϕ obtained using the same procedure adopted in the Si(111) case and a freeze-in temperature of 767 K.[12] $\tilde{\beta}$ grows monotonically as the miscut angle is increased with a tendency to saturate at high angles. Experimentally, the measurements of $\tilde{\beta}$ in the continuous elastic approximation are reliable for vicinalities not larger than 6° since the amplitude of fluctuations of steps is of the order of the step separation; nevertheless the step stiffness at 8° can be extrapolated by a fitting procedure, as discussed below. The relevant experimental data for this surface are listed in Table I.

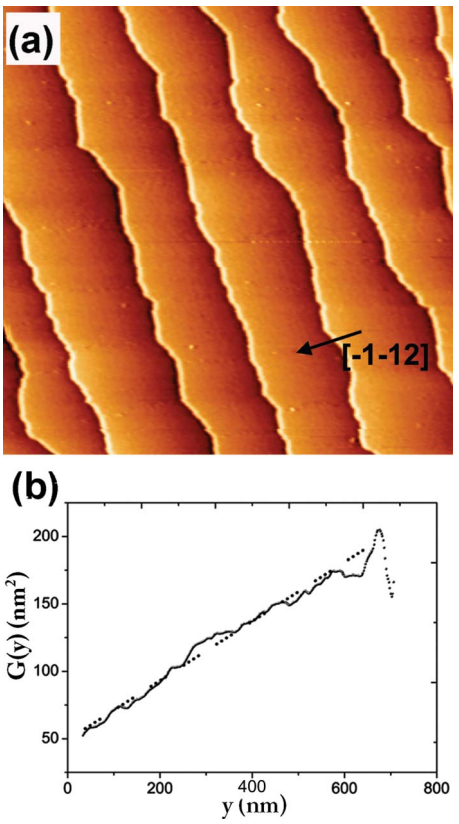

FIG. 2. (Color online) (a) STM image (325×325 nm^2) of the clean Si(111) surface. The direction $[\bar{1}\bar{1}2]$ perpendicular to step edges is evidenced by the arrow. (b) Spatial correlation function $G(y)$ as a function of the coordinate running parallel to step ledges, averaged over 50 steps and a total step length of about 700 nm. The straight dashed line is a fit to the data giving the initial slope of $G(y)$.

V. DISCUSSION

Several papers[18,22,34,35] have described the energetics of steps on vicinal Si(001) surfaces, where the characteristic feature is the occurrence of a step-height transition above a certain miscut angle. Pehlke and Tersoff[19] explained such transition in terms of the step interaction energy, as the miscut angle is increased, more and more pairs of S_A-S_B steps collapse into D_B steps, giving rise to a mixed phase lower in energy than any other combination of pure phases. For a given ϕ, the terrace width $\langle l\rangle$ of a single-stepped surface is half of that of a double-stepped one and the averaged terrace width in the mixed phase can be written as

$$\langle l\rangle=\frac{[n_S(\phi)+2n_D(\phi)]a}{\sqrt{8}\tan\phi}, \tag{5}$$

where $a=0.384$ nm is the surface lattice constant of Si(001) and n_S and n_D are the relative densities of single S_A+S_B and

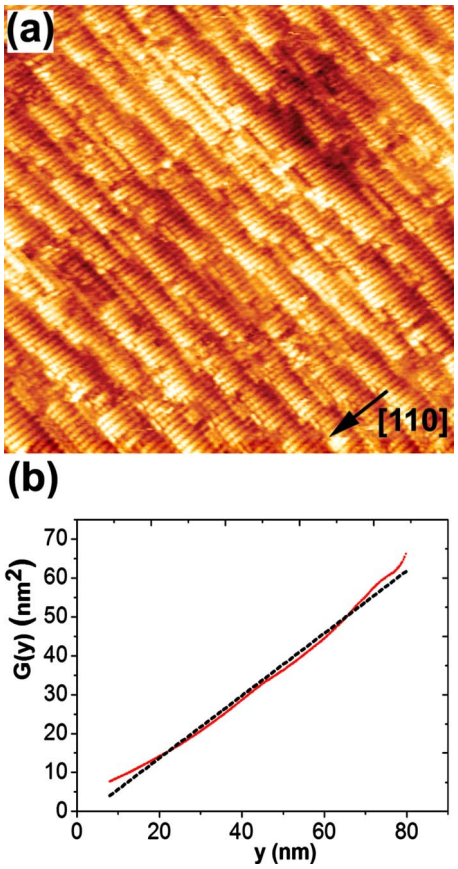

FIG. 3. (Color online) (a) STM image (50×50 nm^2) of the clean 4°-off Si(001) surface. The direction [110] perpendicular to step edges is evidenced by the arrow. (b) Spatial correlation function $G(y)$ as a function of the coordinate running parallel to step edges, averaged over 20 steps and a total step length of about 100 nm. The straight dashed line is a fit to the data giving the initial slope of $G(y)$.

double D_B steps[14] which scale with angle in a complementary fashion. One can see from Fig. 4 that the overall agreement with the calculated curve is excellent and that the average step distance is almost constant at large miscut angles.

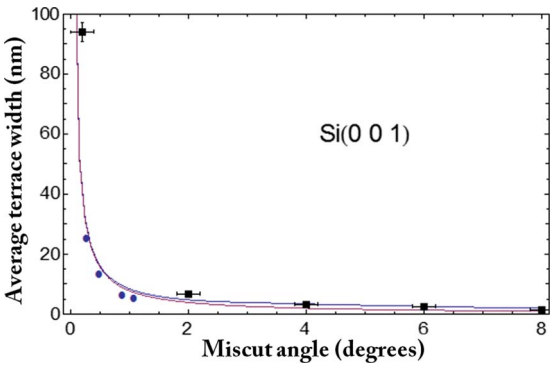

FIG. 4. (Color online) Measured (squares) average terrace widths of mixed (S_A+S_B) and D_B steps as a function of miscut angle for Si(001). The continuos lines are obtained from Eq. (5). The lower curve refers to the S_A+S_B phase only. Full dots are data points taken from Ref. 14.

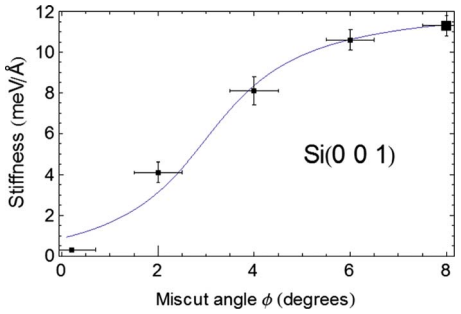

FIG. 5. (Color online) Step stiffness measured at different miscut angles and calculated hyperbolic-sine squared-fitting function of the TSK model. The highlighted point is the extrapolated value of the step stiffness at 8°.

This behavior is characteristic of a mixed phase while the pure single-height S_A+S_B phase decreases more rapidly with increasing the miscut angle. At small misorientation angles an increase in ϕ is accommodated by decreasing the average terrace width. This causes a rise in the interstep interaction energy which makes the steps stiffer, i.e., less likely to undergo wide x fluctuations. At large miscut angles the gradual increase in the stiffness, shown in Fig. 5, is due to the appearance of D_B steps for which bending costs more energy. At this point it is interesting to compare the experimental data with the prediction of the terrace-step-kink model, in which thermal excitation of kinks is the basic cause of the step wandering. According to the TSK model[36] the dependence of $\tilde{\beta}$ on the kink energy ε, taking $a_\perp=a_\parallel=a$, is given by

$$\tilde{\beta}=\frac{2k_BT}{a}\sinh^2\left(\frac{\varepsilon}{2k_BT}\right). \tag{6}$$

By expressing the ε energy in Eq. (6) in terms of the step densities n_S and n_D,[14] one can fit the stiffness data and obtain

TABLE I. Experimental quantities needed to describe Si(001) vicinal surfaces. ϕ is the miscut angle, $\langle l\rangle$ is the average terrace width, σ^2 is the variance of the standardized TWD Gaussian distribution, A is the interaction strengths, and $\tilde{\beta}$ is the step stiffness. The value of the interaction strength A for the quasiflat surface is extracted from the Gaussian TWD; at larger miscut angles, where the harmonic-well approximation breaks down, the values of the interaction strength evaluated from the Gaussian TWD (in brackets) are compared with the values of A calculated from the ground-state energy in case of entropic wandering (not in brackets). Quoted errors are standard errors. The value of the step stiffness at 8° is extrapolated from the fitting curve shown in Fig. 5.

ϕ	$\langle l\rangle$ (nm)	σ^2	A (eV Å)	$\tilde{\beta}$ (meV/Å)
0.2°	94 ± 3	0.022 ± 0.007	636 ± 504	0.30 ± 0.04
2°	6.8 ± 0.2	0.03 ± 0.01	(22 ± 17) 1.3 ± 0.2	4.1 ± 0.5
4°	3.23 ± 0.09	0.018 ± 0.006	(29 ± 20) 0.54 ± 0.03	8.1 ± 0.7
6°	2.52 ± 0.05	0.015 ± 0.003	(41 ± 24) 0.52 ± 0.05	10.6 ± 0.5
8°	1.36 ± 0.02	0.014 ± 0.004	0.47 ± 0.02	$11.3\pm0.5^*$

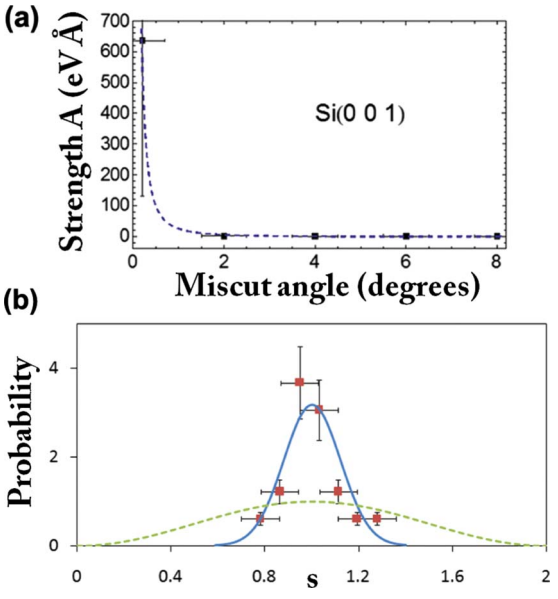

FIG. 6. (Color online) (a) Strength coefficient A for vicinal Si(001) surfaces calculated for a mixed phase of single- and double-height steps using the elastic continuum model and the atomistic calculations of Poon *et al.* The squares are the experimental data obtained using a freeze-in temperature $T=767$ K, in the two limit regimes, i.e., (i) energetic interactions using the measured stiffness and the normalized variance σ^2 of the $\check{P}(s)$ distribution up to $\phi \lesssim 2°$ and (ii) entropic interactions above. In the first case the quoted error comes from the fourth power dependence of σ^2 entering $\tilde{A}$. The value at 8° is evaluated from the extrapolated step stiffness reported in Table I. (b) Experimental (squares) standardized terrace-width distribution of the 4°-off Si(001) surface; the vertical error bars are calculated assuming the relative errors to be $\sqrt{N}/N$, where N is the number of terraces analyzed; the horizontal error bars represent the histogram bin values. The continuous line is the Gaussian fit of the experimental distribution, $\check{P}(s)=\frac{1}{\sigma\sqrt{2\pi}}\exp[-\frac{(s-1)^2}{2\sigma^2}]$. The dashed line is the distribution $\check{P}'(s)=\sin^2[\frac{\pi s}{2}]$ corresponding to entropic step-step repulsion.

the kink energies $\varepsilon_S=20$ meV/atom and $\varepsilon_{\mathrm{DB}}=70$ meV/atom for the S_A+S_B and D_B steps, respectively. The latter energies can be compared to the values $\varepsilon_{\mathrm{SA}}=28\pm2$ meV/atom and $\varepsilon_{\mathrm{SB}}=90\pm10$ meV/atom, measured[37] at 873 K. The goodness of the fit is evident in Fig. 5. The similarity between S_B and D_B energies is not fortuitous since, at high temperatures the meandering weakens the distinction between single and double steps.[17] Moreover the same fitting curve can be used to extrapolate the step stiffness at 8°, which cannot be directly measured.

The experimental interaction strength $A(\phi)$ extracted from TWD fits is in agreement with atomistic calculations only for the quasiflat surface. At larger angles, the harmonic-well approximation overestimates the atomistic data, although the overall functional behavior is preserved (Table I). We point out that for $\phi \geq 2°$ thermal step fluctuations are comparable to the terrace width, thus the main interaction in the GM approximation is the entropic repulsion[38] which hinders step crossing. In this limit, A can be calculated from the ground-state kinetic energy of a 1D infinite square well of width $2\langle l\rangle$, that is,

$$E(\phi)=\frac{(\pi k_B T)^2}{8\tilde{\beta}\langle l\rangle^2}. \tag{7}$$

These values result in excellent agreement with atomistic theory as shown in Fig. 6(a). However the corresponding standardized distribution, $\check{P}'(s)=\sin^2[\frac{\pi s}{2}]$ with $s\in[0,2]$, does not fit the measured terrace-width distributions, as evident in Fig. 6(b). In principle, a closed-form distribution function for repulsive interactions $A\langle l\rangle^{-2}$ could be evaluated by computing the conditional probability of correlated particles (fermions), along the lines described in Ref. 38. In general repulsive interactions tend to sharpen the $\check{P}(s)$ distribution, providing a better description of the experimental data. We stress that there is no evidence whatsoever of any S-to-D crossover angle, which was estimated to occur around 3° at 767 K.[23] This finding is, in general, accord with the phase diagram of the vicinal Si(001) surfaces[39] predicting the critical temperature at 490 K, well below the equilibration temperature used in the present experiment.

VI. CONCLUSION

We have analyzed several vicinal Si(001) surfaces up to 8° in the continuum step approximation. The average terrace width and step stiffness have been measured as a function of the miscut angle by using tunneling microscopy. For a binary mixture of single- and double-height steps, the Gruber-Mullins model has been exploited to compute the interstep interaction strength. This strength is clearly a monotonic function of the miscut angle, which decreases quickly between 0° and 2° and reaches an almost constant value when the angle gets higher, in close agreement with atomistic calculations. No evidence is found of the step-height crossover in line with previous investigations.[18–20]

[1] F. Rosei, J. Phys.: Condens. Matter **16**, S1373 (2004).
[2] J. Zhu, K. Brunner, and G. Abstreiter, Appl. Phys. Lett. **72**, 424 (1998).
[3] V. Ignatescu, J. M. Hsu, A. C. Mayer, J. M. Blakely, and G. G. Malliras, Appl. Phys. Lett. **89**, 253116 (2006).
[4] W. Xiao Pascal Ruffieux, Kamel Aït-Mansour, Oliver Gröning, Krisztian Palotas, Werner A. Hofer, Pierangelo Gröning, and Roman Fasel, J. Phys. Chem. B **110**, 21394 (2006).
[5] F. Leroy, P. Müller, J. J. Métois, and O. Pierre-Louis, Phys. Rev. B **76**, 045402 (2007).
[6] J. J. Metois, A. Saul, and P. Muller, Nature Mater. **4**, 238 (2005).
[7] C. Didiot, S. Pons, B. Kierren, Y. Fagot-Revurat, and D. Malterre, Nat. Nanotechnol. **2**, 617 (2007).
[8] P. D. Szkutnik, A. Sgarlata, A. Balzarotti, N. Motta, A. Ronda,

and I. Berbezier, Phys. Rev. B **75**, 033305 (2007).
[9] M. Bernardi, A. Sgarlata, M. Fanfoni, A. Balzarotti, and N. Motta, Appl. Phys. Lett. **93**, 031917 (2008).
[10] F. Watanabe, D. G. Cahill, S. Hong, and J. E. Greene, Appl. Phys. Lett. **85**, 1238 (2004).
[11] I. Berbezier and A. Ronda, Surf. Sci. Rep. **64**, 47 (2009).
[12] H. C. Jeong and E. D. Williams, Surf. Sci. Rep. **34**, 171 (1999).
[13] E. D. Williams and N. C. Bartelt, Science **251**, 393 (1991).
[14] B. S. Swartzentruber, N. Kitamura, M. G. Lagally, and M. B. Webb, Phys. Rev. B **47**, 13432 (1993).
[15] D. J. Chadi, Phys. Rev. Lett. **59**, 1691 (1987).
[16] A. A. Baski, S. C. Erwin, and L. J. Whitman, Surf. Sci. **392**, 69 (1997).
[17] P. E. Wierenga, J. A. Kubby, and J. E. Griffith, Phys. Rev. Lett. **59**, 2169 (1987).
[18] X. Tong and P. A. Bennett, Phys. Rev. Lett. **67**, 101 (1991).
[19] E. Pehlke and J. Tersoff, Phys. Rev. Lett. **67**, 465 (1991).
[20] T. W. Poon, S. Yip, P. S. Ho, and F. F. Abraham, Phys. Rev. Lett. **65**, 2161 (1990); Phys. Rev. B **45**, 3521 (1992).
[21] V. I. Marchenko, Sov. Phys. JETP **54**, 605 (1981); JETP Lett. **33**, 381 (1981).
[22] O. L. Alerhand, D. Vanderbilt, R. D. Meade, and J. D. Joannopoulos, Phys. Rev. Lett. **61**, 1973 (1988).
[23] T. W. Poon, F. F. Abraham, S. Yip, and P. S. Ho, Europhys. Lett. **16**, 277 (1991).
[24] N. C. Bartelt, T. L. Einstein, and E. D. Williams, Surf. Sci. **240**, L591 (1990).
[25] J. Frohn, M. Giesen, M. Poensgen, J. F. Wolf, and H. Ibach, Phys. Rev. Lett. **67**, 3543 (1991).
[26] C. Alfonso, J. M. Bermond, J. C. Heyraud, and J. J. Métois, Surf. Sci. **262**, 371 (1992).
[27] Y. N. Yang, B. M. Trafas, R. L. Siefert, and J. H. Weaver, Phys. Rev. B **44**, 3218 (1991).
[28] E. E. Gruber and W. W. Mullins, J. Phys. Chem. Solids **28**, 875 (1967).
[29] H. Gebremariam, S. D. Cohen, H. L. Richards, and T. L. Einstein, Phys. Rev. B **69**, 125404 (2004).
[30] A. Sgarlata, P. D. Szkutnik, and A. Balzarotti, Appl. Phys. Lett. **83**, 4002 (2003).
[31] N. C. Bartelt, J. L. Goldberg, T. L. Einstein, E. D. Williams, J. C. Heyraud, and J. J. Métois, Phys. Rev. B **48**, 15453 (1993).
[32] E. D. Williams, R. J. Phaneuf, J. Wei, N. C. Bartelt, and T. L. Einstein, Surf. Sci. **310**, 451 (1994).
[33] C. Schwennicke, X. S. Wang, T. L. Einstein, and E. D. Williams, Surf. Sci. **418**, 22 (1998).
[34] O. L. Alerhand, A. N. Berker, J. D. Joannopoulos, D. Vanderbilt, R. J. Hamers, and J. E. Demuth, Phys. Rev. Lett. **64**, 2406 (1990); **66**, 962 (1991).
[35] N. C. Bartelt, T. L. Einstein, and C. Rottman, Phys. Rev. Lett. **66**, 961 (1991).
[36] N. C. Bartelt and T. L. Einstein, Surf. Sci. **276**, 308 (1992).
[37] B. S. Swartzentruber, Y. W. Mo, R. Kariotis, M. G. Lagally, and M. B. Webb, Phys. Rev. Lett. **65**, 1913 (1990).
[38] T. L. Einstein, Appl. Phys. A: Mater. Sci. Process. **87**, 375 (2007).
[39] E. Pehlke and J. Tersoff, Phys. Rev. Lett. **67**, 1290 (1991).